MRA Evaluation of Intravascular Stents

MRA can be successfully utilized in evaluating intravascular stents, particularly in the case of newer nonferromagnetic stents.

BY KEVIN W. MENNITT, MD, AND JOHN H. RUNDBACK, MD

The majority of atherosclerotic visceral artery stenosis, including that occurring in the renal arteries, is due to ostial plaque formation that requires stent implantation for optimal endovascular treatment. Hemodynamically significant restenosis after stent placement occurs in approximately 11% to 25% of cases.[1] The evaluation of patency after stent placement may be performed using conventional catheter angiography, CTA, or duplex ultrasound. None of these techniques is optimal. Catheter angiography is inherently invasive, and both angiography and CTA require the administration of potentially nephrotoxic radiocontrast. Duplex sonography is operator dependent and often technically difficult due to patient respiration or body habitus.[2]

MRA has emerged as an easily performed and reliable imaging modality for native renal and visceral artery stenosis. However, MR imaging after intravascular stent placement is challenging. The evaluation of stent patency is limited by shielding from radiofrequency signals

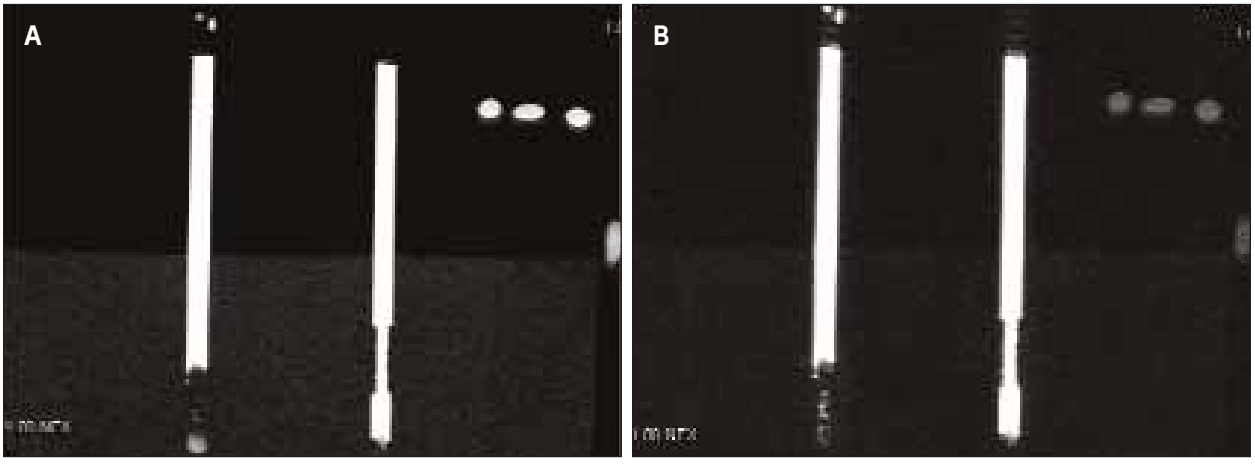

Figure 1. Two images from a three-dimensional (3D) MRI of a phantom (bandwidth, 62.5 kHz; slice thickness, 3 mm). In both images, a stainless steel stent is present on the left, and a cobalt-chromium stent is on the right. Figure 1A was obtained with a flip angle of 20º; Figure 1B was obtained with a flip angle of 60º. Note that on both images, the cobalt-chromium stent has superior in-stent signal. Serial images with increasing flip angles demonstrated that although increasing the flip angle up to 60º increased the signal within the stent, lower flip angles gave acceptable results.

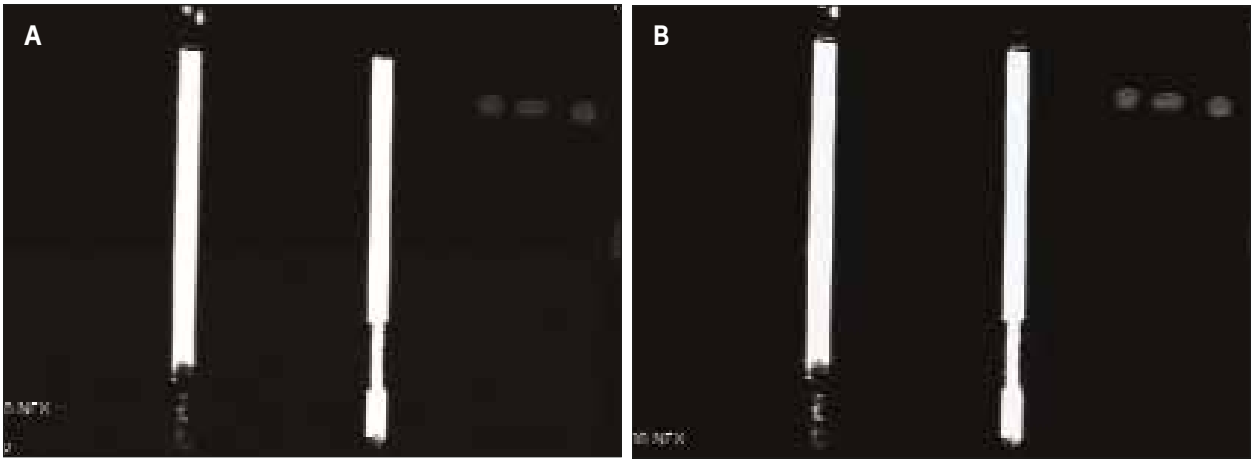

Figure 2. Two images from a 3D MRA of a phantom (stainless steel stent in the tube on the left, and a cobalt-chromium stent in the tube on the right). Figure 2A was obtained with a slice thickness of 2 mm; Figure 2B was obtained with a slice thickness of 3 mm. There is a slightly perceptible improvement in visualization within the cobalt-chromium stent utilizing a smaller slice thickness, which has been confirmed through clinical experience. Minimal signal is seen within the stainless steel stent.

and susceptibility artifacts (ferromagnetic artifact), both of which cause loss of signal both within and adjacent to the stented vessel.[3-12] Ferromagnetic stainless steel stents result in marked image degradation due to local magnetic field heterogeneity, essentially precluding reliable image interpretation.[13]

Although visceral artery stenting has traditionally been performed with stainless steel alloy stents, newer stent designs have emerged during the past several years. Nonferromagnetic stents manufactured of medical-grade cobalt-chromium, platinum, or nitinol are expected to produce less magnetic susceptibility and a markedly reduced degree of MRI image interference than traditional stainless steel alloy, balloon-expandable stents. To study this, we have conducted gadolinium-enhanced MR imaging in both static phantoms and human patients with cobalt-chromium stents (Racer, Medtronic, Santa Rosa, CA) and stainless steel stents (Herculink, Guidant Corporation, Indianapolis, IN) to determine comparative image quality and optimize MR techniques for evaluating stent patency.

MRI PHANTOM

Balloon-expandable cobalt-chromium and stainless steel stents were deployed to 6 mm in diameter in plastic straws filled with 6% gadolinium solution (3 mL in 50 mL saline) and suspended in a gelatin agar phantom model. Sequential coronal images of the phantom were then obtained using variable echo time (TE), flip angle, and slice thickness. Figures 1 and 2 show the effects of varying these imaging parameters on in-stent 3D MR visibility.

CLINICAL IMAGING

Patients who had previously undergone placement of a cobalt-chromium alloy stent in the renal artery or superior mesenteric artery were imaged. Racer stents were used in this series because they were the only balloon-expandable cobalt-chromium stents commercially

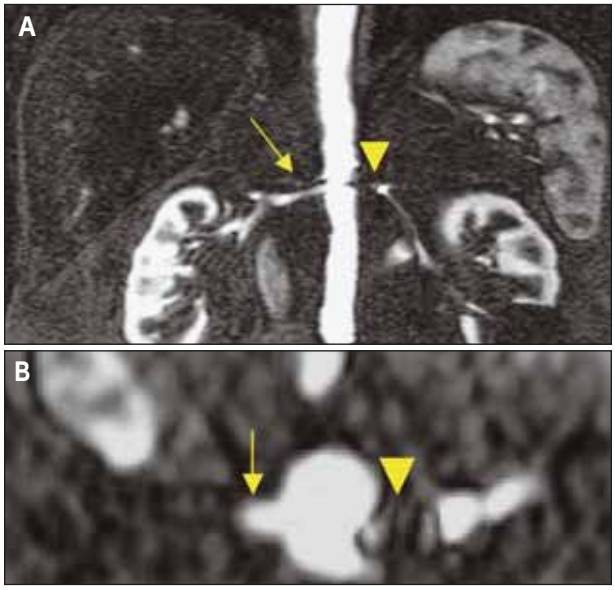

Figure 3. Coronal (A) and axial (B) 3D MRA with flip angle of 60°, slice thickness of 2.6 mm, and TR/TE of 6.9/1.2. A cobalt-chromium stent is present in the proximal right renal artery (arrow) and an NIR Royal stent (Boston Scientific Corporation, Natick, MA) is present in the left renal artery (arrowhead). Note that flow within the stainless steel stent is not visualized. The cobalt-chromium stent is widely patent.

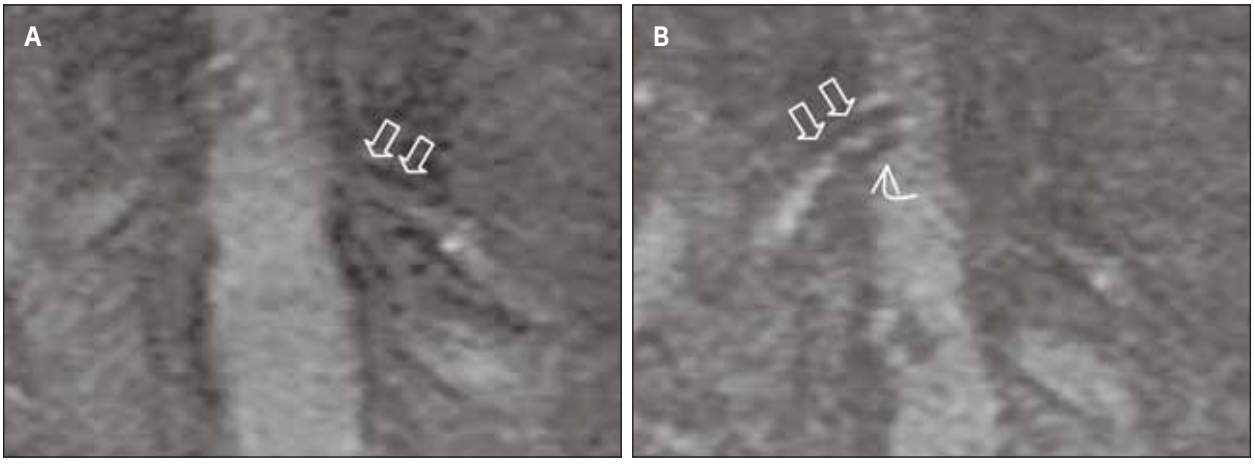

Figure 4. Coronal 3D MRA with a flip angle of 60º, TR/TE of 6.8/1.2, and a slice thickness of 3 mm. These images were obtained with poor gadolinium bolus timing. Despite this, bilateral renal artery cobalt-chromium stent patency is demonstrated on sequential images (open arrows). Figures 3 and 7 illustrate the importance of timing the gadolinium bolus to enhance imaging. Note the minimal stent strut low-signal artifact along the length of the implanted stent (curved arrow in B).

available at the time of the procedures. Some of the patients also had a stainless steel stent implanted in the contralateral renal artery allowing for comparison. Contrast-enhanced MRA imaging was performed after intravenous injection of gadolinium. Fluoro-triggering was utilized to detect the arrival of the gadolinium bolus in the abdominal aorta. Finally, sequential acquisition of k-space was used to decrease the artifact caused by the metallic stent. Images are shown in Figures 3 through 7.

DISCUSSION

MRA is easily performed, operator independent, and is an attractive modality for imaging patients with visceral artery stenosis. However, traditionally utilized stainless steel stents preclude effective MR imaging due to signal loss caused by magnetic susceptibility effects and Faraday shielding.[3-5,7] Although more recently available nonferromagnetic stents do not produce signal loss from magnetic susceptibility, shielding effects may still degrade image quality. To achieve optimal imaging, imaging parameters may be adjusted to enhance in-stent signal.[4,10] The impact of varying different MR parameters is shown in Table 1.

Three-dimensional gadolinium-enhanced MRA generally employs short TR (repetition time) and TE.[12] To minimize dephasing, the shortest possible TE should be used, with a bandwidth generally of 62.5 kHz. Additionally, to overcome some of the radiofrequency shielding limitations imposed by a stent, a high flip-angle (usually 60º) is needed. A small slice thickness (typically 2 mm to 3 mm) should be used to increase resolution.[8]

In most of our clinical cases, 40 mL of gadolinium was injected. Fluoro-triggering was utilized to detect the arrival of the gadolinium bolus in the abdominal aorta. Finally, sequential acquisition of k-space was used to decrease the artifact caused by the metallic stent. Imaging during the peak of gadolinium enhancement, using either fluoro-triggering or automatic bolus detection (such as SmartPrep, GE Healthcare, Waukesha, WI) is necessary for image optimization. Additionally, sequential ordering of k-space limits ringing artifact, which results when imaging starts too early.

Three-dimensional MRA should be obtained in the plane that limits the number of slices (to decrease time and breath-hold) but covers the entire area of interest.

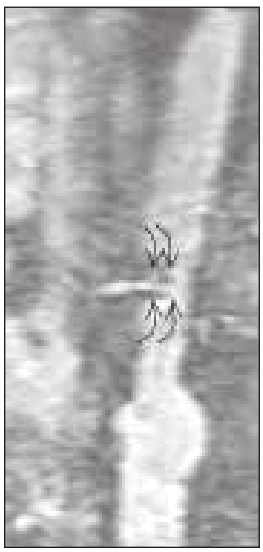

Figure 5. Sagittal 3D MRA (coronal reconstruction shown). This patient had a solitary right renal artery that was stenotic and was treated with angioplasty and cobalt-chromium stent placement. MRA imaging was obtained in the sagittal plane rather than the usual protocol of acquisition parallel to the stent in the coronal plane with subsequent axial and sagittal image reconstruction. This results in greater stent edge image degradation (curved black arrows).

TABLE 1. FACTORS AFFECTING IN-STENT MRI

Parameter	Effect on MRA
Stent material	Variable
Stent thickness, strut geometry	Variable
Echo time	Shorter improves image
Repetition time	Shorter decreases breath-hold
Flip angle	Longer improves image
Bandwidth	Longer improves image
Slice thickness	Thinner improves image
Gadolinium bolus (injection rate, MR triggering)	Tighter bolus improves image
Plane of image acquisition	Parallel to stent improves image

We have found that reading 3D MRA on a workstation is optimal because it allows quick and easy reconstructions in multiple planes. In our clinical practice, we utilize the MRA parameters listed in Table 2 to obtain high-quality diagnostic images.

The cobalt-chromium stent used in these studies produced diagnostic images in the majority of cases, despite incomplete acquisition optimization in several instances. Flow lumen images produced were superior in all cases to those seen with stainless steel stents. Understanding the MRI strategies to maximize in-stent visualization should allow quality MRI of cobalt-chromium stents in most patients.

The Racer stent was used in this study because it was the only commercially available cobalt-chromium platform at the time of investigation. Recently, another cobalt-chromium stent has become available (Palmaz Blue, Cordis Corporation, a Johnson & Johnson company, Miami, FL). In addition, there are various stents composed of nitinol and platinum alloys, which are also non-ferromagnetic. Although we have not evaluated the MRI transparency of each of these stents in either an MR phantom or clinical setting, other investigators have suggested that platinum stents have a low shielding effect and few MR artifacts.[12] However, because image qual-

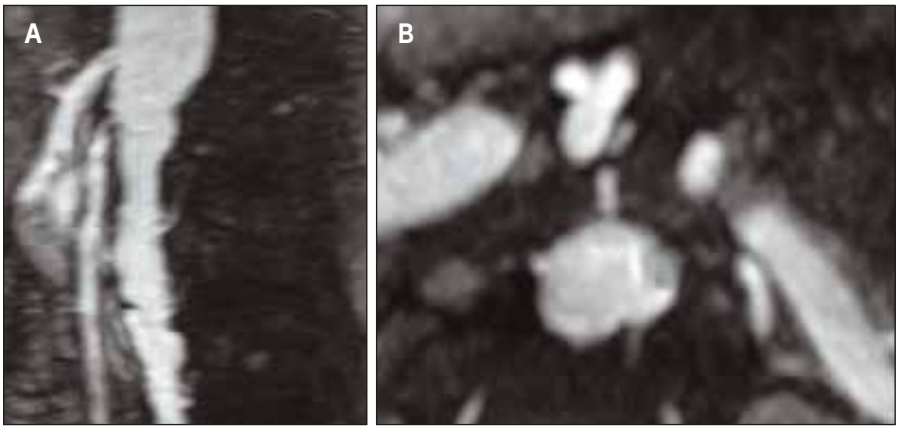

Figure 6. Three-dimensional MRA of the SMA after cobalt-chromium stent placement. MRA imaging was obtained in the coronal plane; Figure 6A depicts the data set in the sagittal plane, whereas Figure 6B depicts the axial plane. Note that the axial images demonstrate a widely patent SMA lumen within the stent. In this case, sagittal acquisition of the 3D MRA would have been optimal because the SMA lies in a sagittal plane. This further illustrates the importance of viewing and interpreting the MRA on a workstation that allows for multiplanar reconstructions.

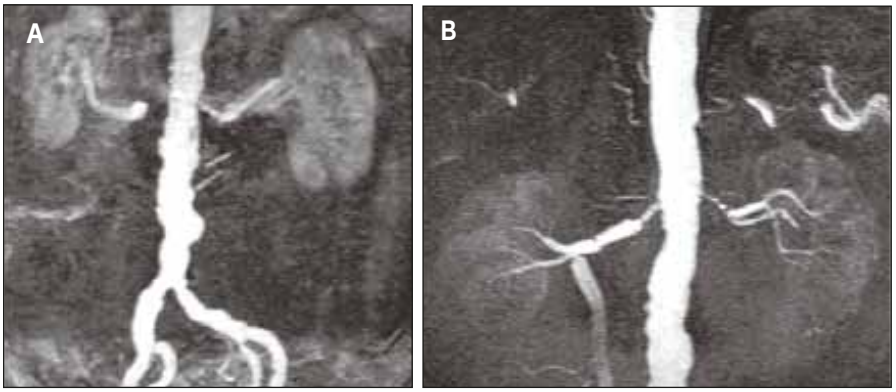

Figure 7. Three-dimensional coronal MRAs from two patients. Figure 7A depicts a Genesis stent (Cordis Corporation, a Johnson & Johnson company, Miami, FL) in the right renal artery and a cobalt-chromium stent in the left renal artery. Figure 7B depicts a cobalt-chromium stent in the right renal artery and a stainless steel stent in the left renal artery. Both images demonstrate superior visualization of the vessel lumen within the cobalt-chromium stent compared to the contralateral side. Time-resolved imaging may be used to further assess stent patency and renal flow.

ity can be affected by a variety of factors other than the metal alloy employed, it is difficult to predict the ability of MRA to accurately image current clinically utilized visceral stents. Rather, the comparative effect of stent composition and geometry on MR image quality needs to be prospectively evaluated in future preclinical and patient models.

CONCLUSION

In summary, MRA of stented vessels can be successfully performed, particularly when nonferromagnetic stents are present. It is essential to identify patients with intravascular stents prior to MRI so that the protocol can be optimized. By changing the MRA parameters, high-quality imaging can be achieved. ■

TABLE 2. MRA OF INTRAVASCULAR STENTS AT 1.5T

Contrast	40 mL gadolinium chelate
Injection rate	3-5 mL/s with 40-mL saline flush
Sequence	3D fast spoiled gradient echo Minimum TR/TE Slice thickness 2-3 mm Bandwidth 62.5 kHz or higher Flip angle 60º-75º

Note: Use of MR fluoro-triggering or automatic bolus detection should be utilized to optimize contrast imaging.

Kevin W. Mennitt, MD, is Chief of Body MRI, Assistant Professor of Radiology, Weill Medical College of Cornell University, New York. He has disclosed that he is a paid consultant for Medtronic. Dr. Mennitt may be reached at kem9003@med.cornell.edu.

John H. Rundback, MD, is Director, Interventional Radiology, Holy Name Hospital, and Associate Professor of Radiology, Columbia University College of Physicians and Surgeons, Teaneck, New Jersey. He has disclosed that he is a paid consultant for Medtronic. Dr. Rundback may be reached at jr2041@columbia.edu.

1. Safian RD, Textor SC. Renal artery stenosis. N Engl J Med. 2001;344:431-442.
2. Lee HY, Grant EG. Sonography in renovascular hypertension. J Ultrasound Med. 2002;21:431-441.
3. Bartels LW, Smits HF, Bakker CJ, et al. MR imaging of vascular stents: effects of susceptibility, flow, and radiofrequency eddy currents. J Vasc Interv Radiol. 2001;12:365-371.
4. Spuentrup E, Ruebben A, Stuber M, et al. Metallic renal artery MR imaging stent: artifact-free lumen visualization with projection and standard renal MR angiography. Radiol. 2003;227:897-902.
5. Maintz D, Kugel H, Schellhammer F, et al. In vitro evaluation of intravascular stent artifacts in three-dimensional MR angiography. Invest Radiol. 2001;36:218-224.
6. Maintz D, Tombach B, Juergens KU, et al. Revealing in-stent stenoses of the iliac arteries: comparison of multidetector CT with MR angiography and digital radiographic angiography in a phantom model. AJR. 2002;179:1319-1322.
7. Lenhart M, Völk M, Manke C, et al. Stent appearance at contrast-enhanced MR angiography: in vitro examination with 14 stents. Radiol. 2000;217:173-178.
8. Meyer JM, Buecker A, Schuermann K, et al. MR evaluation of stent patency: in vitro test of 22 metallic stents and the possibility of determining their patency by MR angiography. Invest Radiol. 2000;35:739-746.
9. Prince MR, Narasimham DL, Stanley JC, et al. Breath-hold gadolinium-enhanced MR angiography of the abdominal aorta and its major branches. Radiology. 1995;197:785-792.
10. Van Holten J, Wielopolski P, Bruck E, et al. High flip angle imaging of metallic stents: implications for MR angiography and intraluminal signal interpretation. Magn Reson Med. 2003;50:879-883.
11. Wang Y, Truong TN, Yen C, et al. Quantitative evaluation of susceptibility and shielding effects of nitinol, platinum, cobalt-alloy, and stainless steel stents. Magnet Reson Med. 2003;49:972-976.
12. Trost DW, Zhang HL, Prince MR, et al. Three-dimensional MR angiography in imaging platinum alloy stents. J Magn Reson Imag. 2004;20:975-980.
13. Teitelbaum GP, Bradley WG Jr, Klein BD. MR imaging artifacts, ferromagnetism, and magnetic torque of intravascular filters, stents, and coils. Radiology. 1988;166:657-664.